JOURNAL OF MATERIALS SCIENCE **38** (2003) 3641 – 3646

Atomic force microscopy (AFM) study on potassium hexatitanate whisker ($K_2O{\cdot}6TiO_2$)

JINGWEI XIE, XIAOHUA LU*, YU ZHU, CHANG LIU, NINGZHONG BAO, XIN FENG
Department of Chemical Engineering, Nanjing University of Technology, Nanjing, Jiangsu, 210009, People's Republic of China
E-mail: xhlu@njuct.edu.cn

Since potassium hexatitanate whisker is often used for the filler of composites or as a catalyst, its surface is very important. In this paper the surface morphology and structure of potassium hexatitanate fiber has been observed by AFM. The potassium hexatitanate fiber shows that its surface has different "lamellas". In addition, we obtained the temperature dependence of the linear expansive ratios along a, b, c 3 directions of the cell by molecular dynamics simulation. The simulation result shows that the linear expansive ratios along the 3 directions are almost the same. Therefore, the periodical surface structure is not generated by the shrinkage along 3 directions in the cooling process of the $K_2O{\cdot}6TiO_2$ whisker preparation. The surface structure is believed to be related to the mechanism of crystal growth of the $K_2O \cdot 6TiO_2$ whisker and is consistant with the "liquid melt inducing" model [22].

1. Introduction

The annual number of papers showing applications of atomic force microscopy (AFM) to oxides has more than doubled from 1994 to 1997 [1], and from 1997 to 2001 the annual number of papers has also increased sharply. The studies of oxides by AFM concentrated on the following three aspects: the surface of single crystal oxides; the film of oxides and the powdered sample of oxides. However, relatively fewer results on powdered samples have been reported [2–4]. The main reason is that it is difficult to prepare the powdered samples and obtain the high resolution image, especially atomic level resolution. Also, it is not very easy to explain the images obtained. However, the powdered oxides dominate in practice. If the problems mentioned above are overcome, the AFM study on powdered oxides will be very promising.

Since the synthesis cost of $K_2O{\cdot}6TiO_2$ is low and the quality and the cost performance are high, it is widely used. It is well known that the properties of materials are

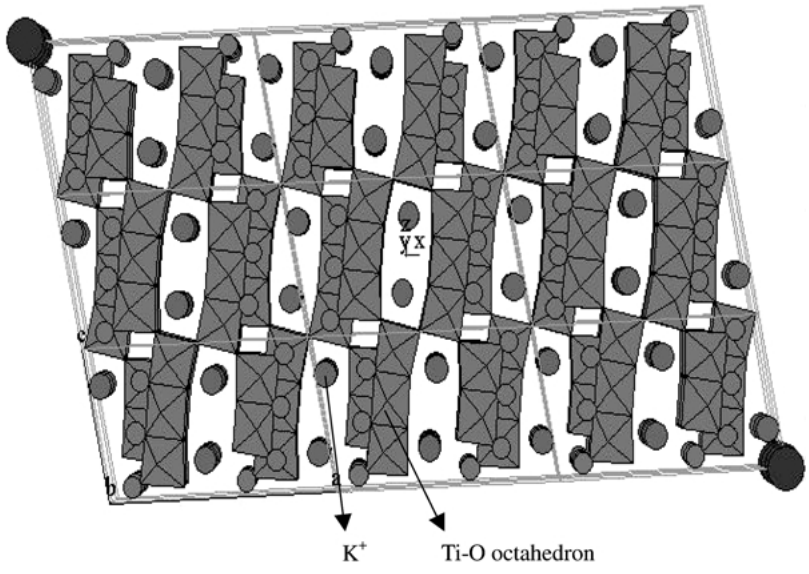

Figure 1 Projection of idea $K_2O \cdot 6TiO_2$ whiskers [010] surface.

*Author to whom all correspondence should be addressed.

determined by the structure of materials. Similarly, the properties of $K_2O \cdot 6TiO_2$ whisker are also determined by its structure. The bulk structure of potassium hexatitanate fiber has been examined in detail by XRD and TEM (SAED) methods [5, 6]. It has a tunneling structure and consists of distorted Ti─O octahedrons, which share the planes and edges and enclose the potassium ions (as show in Fig. 1). Because potassium ions in $K_2O \cdot 6TiO_2$ whisker are enclosed by the tunneling structure and isolated from the environment, potassium ions can't escape from the tunneling structure in the solution and present the inertia of chemistry [5, 7]. It was reported that the axial direction of the $K_2O \cdot 6TiO_2$ whisker along [010] direction was proved by the experiment of TEM (SAED pattern) (see Fig. 1) [5]. Potassium hexatitanate ($K_2O \cdot 6TiO_2$) fiber is an advanced reinforcing material for the composites to improve the property of mechanics and tribology in industry [8–13].

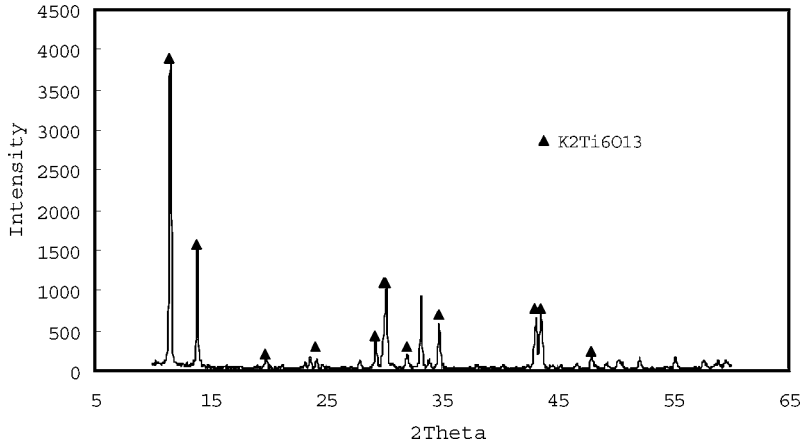

Figure 2 XRD figure of $K_2O \cdot 6TiO_2$ whiskers.

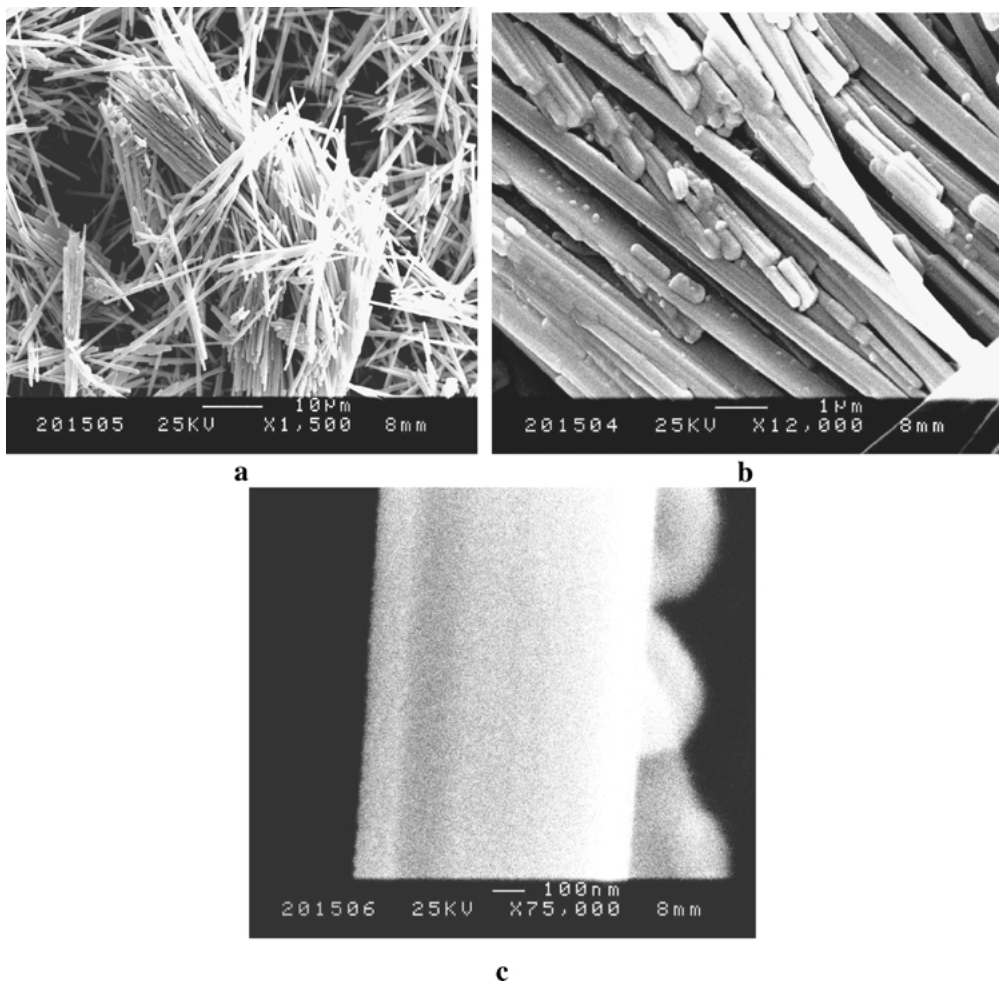

Figure 3 a, b, c are the $K_2O \cdot 6TiO_2$ whiskers SEM pictures of different amplified factors.

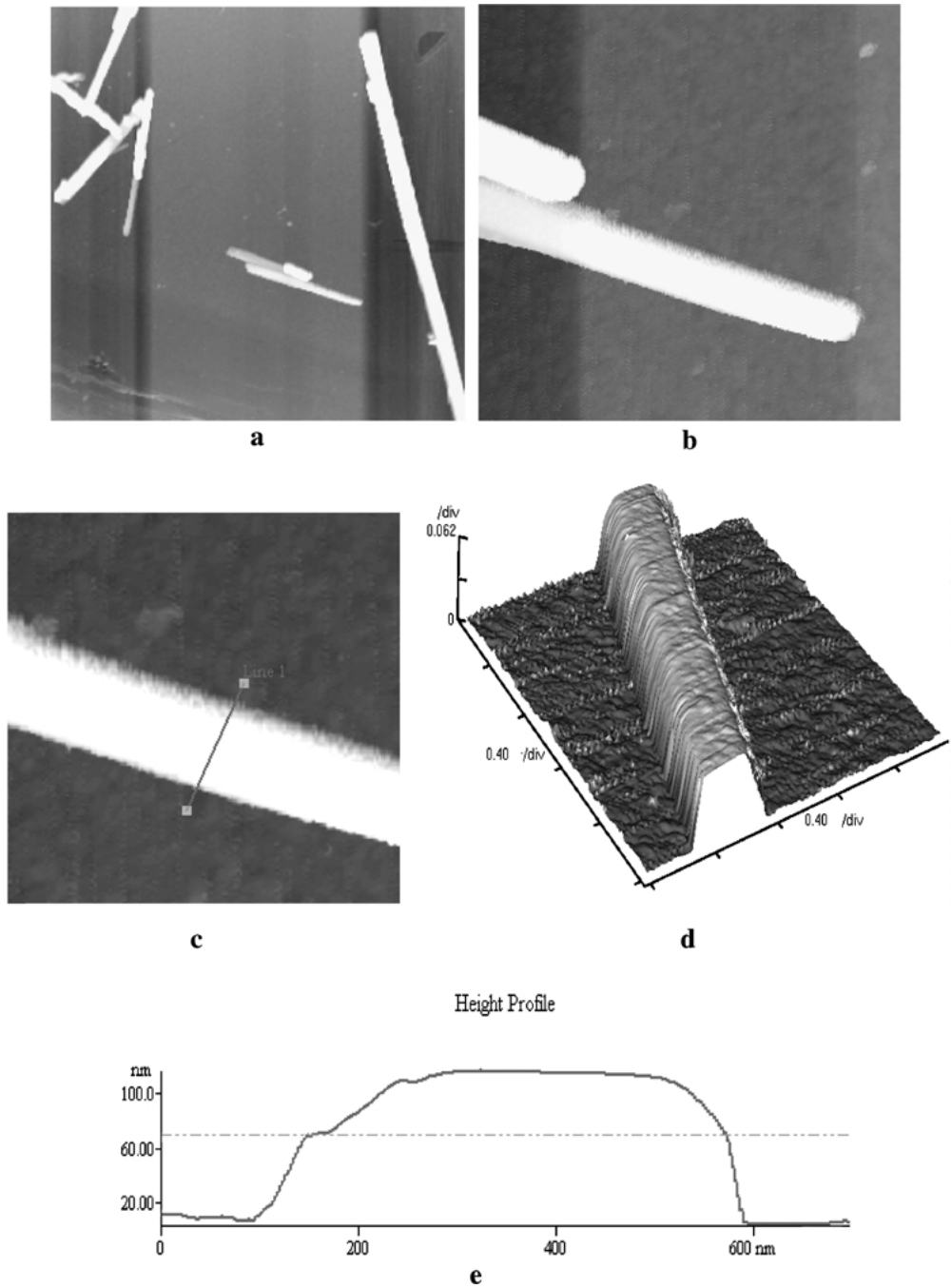

Figure 4 AFM morphology pictures of potassium hexatitanate whisker: (a) 20 μm $\times$ 20 μm (Topography), (b) 4 μm $\times$ 4 μm (Topography), (c) 1800 nm $\times$ 1800 nm (Topography), (d) 3-dimensional picture of Fig. 4c (an angle rotated), and (e) contour of line 1 in Fig. 4c.

Furthermore, fiber-shaped materials have photocatalized characterization [14]. The surface of tunneling structure $K_2O \cdot 6TiO_2$ whisker combined with RuO_2 was used as a photocatalysis for water decompositon [15–17].

Since it is often used as the support, catalyst, advanced reinforcing material for the composites, the modified surface is often required. And the start point of modified surface study is based on the understanding of the surface. The surface morphology and structure of potassium hexatitanate fiber were characterized by SEM and TEM in the past. However, SEM provides too low resolution to observe the details of the surface. Because the diameter of potassium hexatitanate is about 0.3–1 μm and the length is about 3–20 μm, TEM can't be used to observe it directly although the SAED pattern gives the structure of the lattice. Therefore, in this paper we want to observe the morphology and surface structure of potassium hexatitanate $K_2O \cdot 6TiO_2$ whiskers by AFM which can obtain image form micron level to atomic resolution. Also, we want to obtain the local roughness of potassium hexatitanate $K_2O \cdot 6TiO_2$ whiskers, which affects the harm in biology [21].

2. Experimental section

2.1. Materials

The synthetic methods of the fibrous potassium hexatitanate ($K_2O \cdot 6TiO_2$) were reported [18–20]. K_2CO_3 and TiO_2 were mixed up as the raw materials and sintered at a certain temperature. $K_2O \cdot 6TiO_2$ whiskers

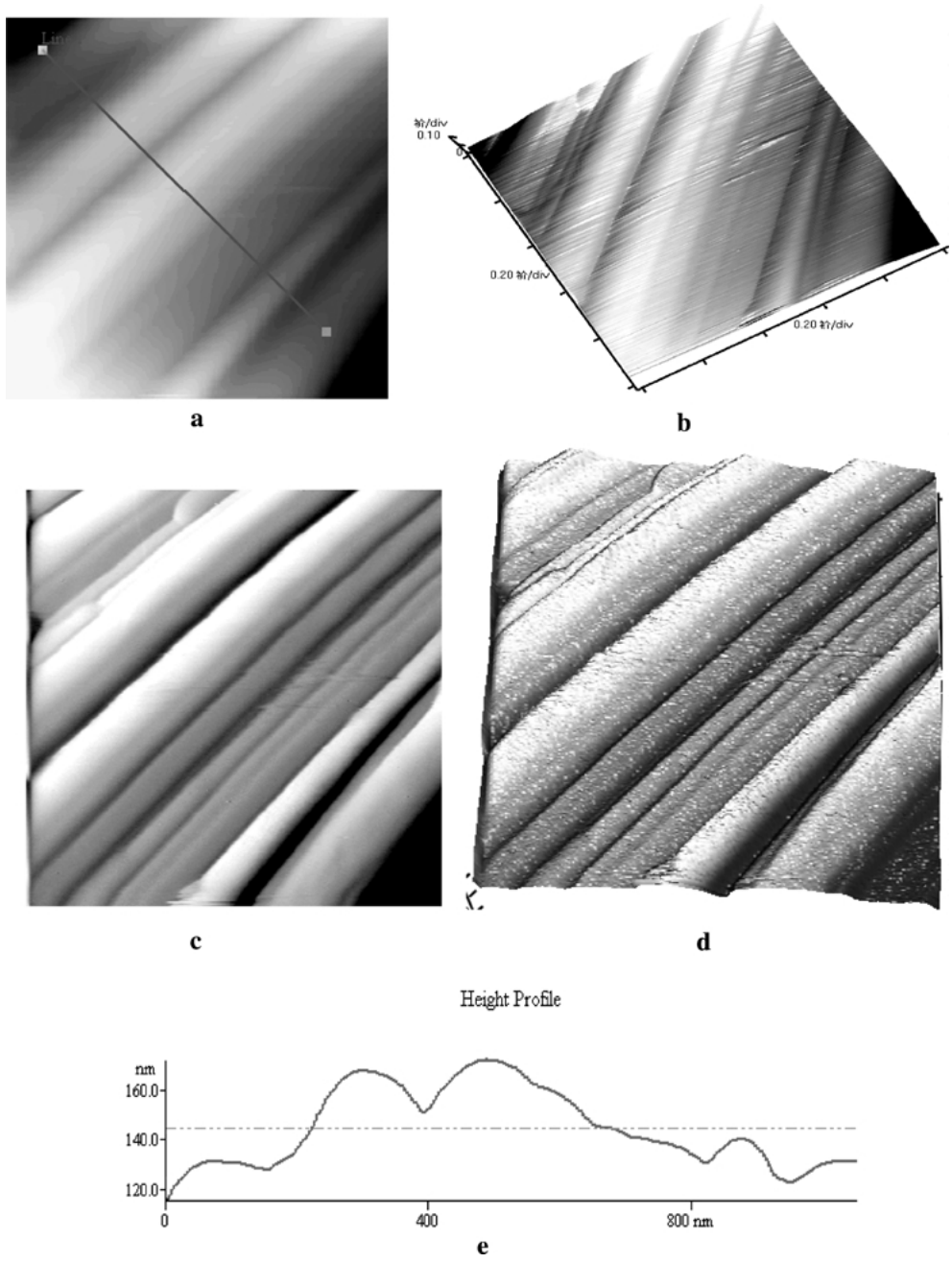

Figure 5 AFM surface structure pictures of potassium hexatitanate whisker: (a) Size: 1000 nm × 1000 nm (Topography), (b) 3-dimensional picture of Fig. 5a, (c) size: 1000 nm × 1000 nm (error signal) the same area with Fig. 5a, (d) 3-dimensional picture of Fig. 5c, and (e) contour of the line in Fig. 5a.

can be obtained directly [22]. Also, $K_2O \cdot 6TiO_2$ whiskers can be obtained by ion-exchange method from intermediate product $K_2O \cdot 4TiO_2$ whiskers [18]. In this paper, the $K_2O \cdot 6TiO_2$ whiskers used are the products of HT300 Japan. Fig. 2. shows the XRD diagram of the $K_2O \cdot 6TiO_2$ whiskers. Fig. 3 shows the SEM pictures of different amplifications of $K_2O \cdot 6TiO_2$ whiskers.

2.2. Atomic force microscopy imaging

The samples used for atomic force microscopy (AFM) observation were prepared by dispersing some products in distilled water followed by ultrasonic vibration for half an hour, then dripping a drop of the dispersion onto a cover glass [4].

Atomic force microscopy (Park Company, Auto Probe CP5 Research) was used to image each sample in air at room temperature. A silicon nitride cantilever with a force constant of 0.26 N/m was used in contact mode AFM. The cantilever was 180 μm long, 25 μm wide and 0.10 μm thick with an attached tip whose apex radius was less than 15 nm. The scan rate is 0.5–3 Hz. Firstly, The sample was placed on the scanner, and some areas contained fibers were found by optical microscopy and monitor. Secondly, we scanned in large areas and found single fiber. Lastly, we scanned the surface of the single fiber with different scan areas.

3. Results and discussions

3.1. Morphology

We chose the 100 μm scanner owing to the size of $K_2O \cdot 6TiO_2$ whisker. The AFM morphology pictures of potassium hexatitanate whisker are given in Fig. 4.

Fig. 4a shows the AFM image (20 μm $\times$ 20 μm Topography) of $K_2O \cdot 6TiO_2$ whiskers deposited on the substrate. Fig. 4b shows the AFM image (4 μm $\times$ 4 μm Topography) of one fraction in Fig. 4a. Fig. 4c shows the single whisker image (1800 nm $\times$ 1800 nm Topography). Fig. 4d shows the 3-dimensional image of Fig. 4c. From Fig. 4d and e we find that the arrises do exist, which present that $K_2O \cdot 6TiO_2$ whisker is a pillar-like crystallite and the cross section is not square [21] but rectangular. Since 3-dimensional images in real space can be obtained by AFM, the images in Fig. 4c and d are more directly perceived through the sense comparing with Fig. 3c.

3.2. Surface structure

The surface of another single $K_2O \cdot 6TiO_2$ whisker was scanned with 5 μm scanner. Fig. 5 shows the surface AFM image (1000 nm $\times$ 1000 nm Topography) of single $K_2O \cdot 6TiO_2$ whisker. From Fig. 5a we find that many lamellas do exist along the axis. Also, we find that the SEM image (Fig. 3b) of a bundle of whiskers is similar to the surface image of a single whisker. Therefore, the surface of the $K_2O \cdot 6TiO_2$ whisker is believed to be composed of many small lamellas and the diameters of the lamellas are about 30 nm–150 nm and these lamellas have the same axial direction with the whisker itself. The surface structure is believed to be related to the crystal growth mechanism of the $K_2O \cdot 6TiO_2$ whisker and coincide with the "liquid melt inducing" model [22]. The model includes 4 processes. In the first process, the surfactant is used to assembly the well-mixed precursor, the anatase-K_2CO_3 inclusion containing the nano TiO_2 powders coated by K_2CO_3 crystallized from the solution. In the second process, the decomposable $K_2Ti_2O_5$ single crystals providing the matrix materials for the formation of $K_2Ti_4O_9$ whiskers are generated by the solid-solid sinter calcination. In the third process, the orientation melt of the K_2O-rich liquid melt splits the decomposable $K_2Ti_2O_5$ single crystals into layer-by-layer $K_2Ti_4O_9$ whiskers with layered crystal structure. Liquid melt covers on the whisker surface to form the sinters with sheaf whisker structure. In the last process, it is processed at a higher reaction temperature. The K_2O-rich liquid melt melts and aggregates in the splits and the spaces among solid $K_2Ti_6O_{13}$ whiskers. When comparing with the third process the whiskers with tunnel crystal structure evolves from the former $K_2Ti_4O_9$ whiskers with layered crystal structure and much more liquid melt generated induces the size decrease of the $K_2Ti_6O_{13}$ whiskers in diameter. Because the atomic resolution images of the $K_2O \cdot 6TiO_2$ whisker haven't been obtained yet, we are not sure which planes the surfaces of $K_2O \cdot 6TiO_2$ whisker are. Because the (100) and $20\bar{1}$ plane are the two weakest binding planes [6], the surface of the $K_2O \cdot 6TiO_2$ whisker perhaps consists of these two planes. Fig. 4b is the 3-dimensional image of Fig. 6a and we find the lamellas clearly. Fig. 5c is the AFM image (Error Signal) the same area as Fig. 5a. Fig. 5d is the 3-dimensional image of Fig. 5c. And the surface structure are seen more clearly from Fig. 5c and d. Fig. 5e shows the contour of the line in Fig. 5a. The Table I gives the line analysis of the line in Fig. 5a. The roughness

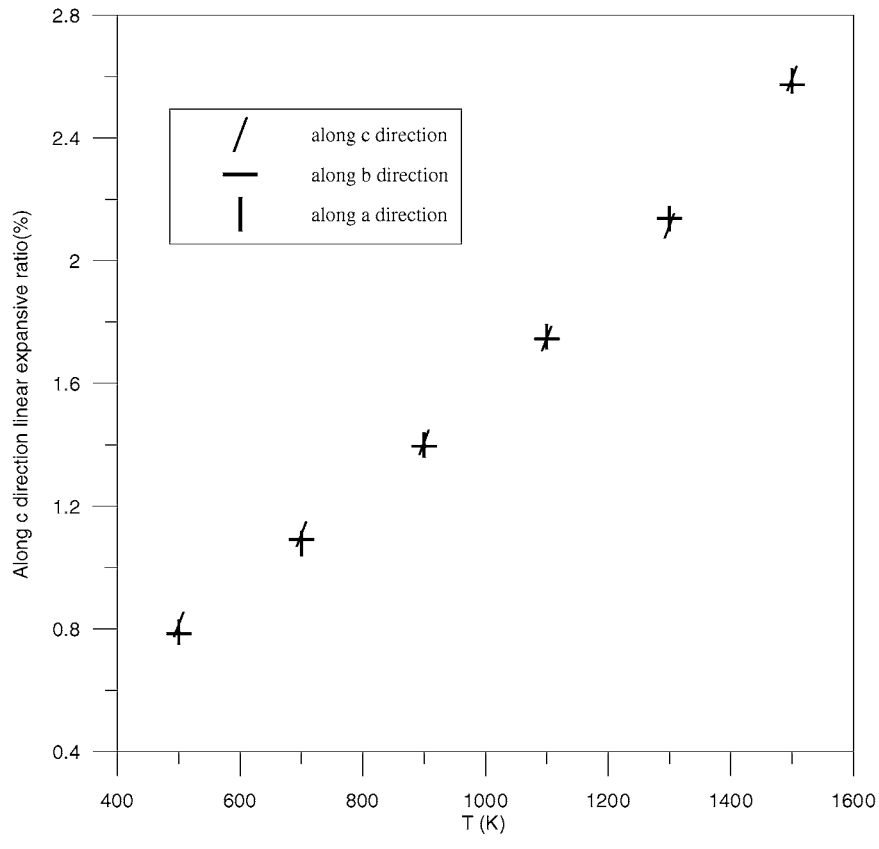

Figure 6 Temperature dependence of linear expansion ratio from molecular dynamics simulation.

TABLE I Line analysis of line 1 in Fig. 5a

Rp-v	Rms rough (Rq)	Rave rough (Ra)	Mean Ht	Median Ht
Line 1 56.84 nm	15.81 nm	14.08 nm	145.6 nm	140.9 nm

along the line in Fig. 5a is about 14.08 nm. It is one of the reasons that the $K_2O \cdot 6TiO_2$ whisker presents weak toxicity. Also, it is the reason that it tends to substitute the asbestos.

4. Molecular dynamics simulation

Molecular dynamics simulation was done on the bulk $K_2Ti_6O_{13}$. The simulation detail could be found in another paper [23]. The simulation results of rutile TiO_2 are in very good agreement with experimental data. The thermal expansivity of $K_2Ti_6O_{13}$ is firstly obtained by molecular dynamics simulation [23]. In this paper Fig. 6 shows the result of simulations-Temperature dependence of linear expansion ratio along a, b, c directions of the cell. The molecular dynamics simulation results show that the linear expansive ratios along three directions are almost the same. Therefore, it is concluded that the periodical surface structure is not generated by the shrinkage along 3 directions in the cooling process of the $K_2O \cdot 6TiO_2$ whisker preparation.

5. Conclusions

In this paper the morphology and the surface structure of the $K_2O \cdot 6TiO_2$ whisker were studied by AFM. The images which resolution is between SEM and SAED pattern of TEM were obtained. In large scan area we obtained the image of the morphology of a single $K_2O \cdot 6TiO_2$ whisker, which presents that it has pillar-like crystallites. The images obtained by AFM are more clearly than SEM pictures. In small scan areas we obtained the image of the surface structure of a single $K_2O \cdot 6TiO_2$ whisker, which presents that the surface has many lamellas. The molecular dynamics simulation results show that the linear expansion ratios along three directions are almost the same. The periodical surface structure is not generated by the shrinkage along three directions in the cooling process of the $K_2O \cdot 6TiO_2$ whisker preparation. The surface structure is believed to be related to the mechanism of crystal growth of the $K_2O \cdot 6TiO_2$ whisker and is consistant with the "liquid melt inducing" model [22].

Acknowledgments

Authors thank the Outstanding Youth Fund of National Natural Science Foundation of P.R. China (29925616), The National High Technology Research and Development Program of China (2003AA333010), and Natural Science Foundation of P.R. China (20246002, 20236010).

References

1. E. M. GAIGNEAUX, *Curr. Opin. Solid State & Mater. Sci.* **3** (1998) 343.
2. J. P. JALAVA, L. HEIKKILA, O. HOVI, R. LAIHO, E. HILTUNEN, A. HAKANEN and H. HARMA, *Ind. Eng. Chem. Res.* **37** (1998) 1317.
3. G. T. K. FEY, K. S. CHEN, B. J. HWANG and Y. L. LIN, *J. Power Sources* **68** (1997) 519.
4. S. YAMAMOTO, O. MATSUOKA and I. FUKADA, *J. Catal.* **159** (1996) 401.
5. B. S. ANDERSSON and A. D. WADSLEY, *Acta Cryst.* **15** (1962) 194.
6. C. L. LI, M. LIU and G. H. WANG, *J. Mater. Res.* **16** (2001) 3614.
7. K. L. BERRY, V. O. AFTANDILIAN, W. W. GILBERT, E. P. H MEIBOHM and H. S. YOUNG, *J. Inorg. Nucl. Chem.* **14** (1960) 231.
8. J. LÜ and X. LU, *J. Appl. Polym. Sci.* **82** (2001) 368.
9. W. JIANG and S. C. TJONG, *Polym. Degrad. Stab.* **66** (1999) 241.
10. S. C. TJONG and Y. Z. MENG, *Polymer* **40** (1999) 1109.
11. S. Q. WU, Z. S. WEI and S. C. TJONG, *Composites Sci. and Tech.* **60** (2000) 2873.
12. S. C. TJONG and Y. Z. MENG, *Polymer* **39** (1998) 5461.
13. S. J. KIM, M. H. CHO, D. S. LIM and H. JANG, *Wear* **251** (2001) 1484.
14. Z. YANG, N. BAO, X. FENG, J. XIE and X. LU, *Chem. J. Chinese Univers.* **23** (2002) 1371.
15. R. B. YAHYA, H. HAYASHI, T. NAGASE, T. EBINA, Y. ONODERA and N. SAITOH, *Chem. Mater.* **13** (2001) 842.
16. S. OGURA, M. KOHNO, K. SATO and Y. INOUE, *Phys. Chem. Chem. Phys.* **1** (1999) 179.
17. S. OGURA, M. KOHNO, K. SATO and Y. INOUE, *Appl. Surf. Sci.* **121/122** (1997) 521.
18. N. BAO, X. LU, X. JI, X. FENG and J. XIE, *Fluid Phase Equilibria* **193** (2002) 229.
19. G. L. LI, G. H. WANG and J. M. HONG, *Mater. Res. Bull.* **34** (1999) 2341.
20. J. H. CHOY and Y. S. HAN, *Mater. Lett.* **34** (1998) 111.
21. MARIKO ONO-OGASAWARA and NORIHIKO KOHYAMA, *Ann. Occup. Hyg.* **43** (1999) 505.
22. N. BAO, X. FENG, X. LU and Z. YANG, *J. Mater. Sci.* **37** (2002) 3035.
23. Y. ZHU, W. JUN, X. LU, H. DING, Y. WANG and J. SHI, *Chinese J. Chem. Eng.* **11** (2003) 170.

Received 26 June 2002
and accepted 5 June 2003